DOI: 10.1002/ejic.200600708

New Dinuclear Mn^{III} Compounds with 2-MeC_6H_4COO and 2-FC_6H_4COO Bridges – Effect of Terminal Monodentate Ligands (H_2O, ClO_4^- and NO_3^-) on the Magnetic Properties

Gema Fernández,[a] Montserrat Corbella,*[a] Gabriel Aullón,[a] Miguel A. Maestro,[b] and José Mahía[c]

Keywords: Manganese / Magnetic properties / Ligand effects

Four new dinuclear Mn^{III} complexes with the general formula $[\{Mn(bpy)L\}(\mu\text{-}RCOO)_2(\mu\text{-}O)\{Mn(bpy)L'\}]^{n+}$ (bpy = 2,2′-bipyridine) have been synthesized with RCOO = 2-MeC_6H_4COO (**1**, **2**) and 2-FC_6H_4COO (**3**, **4**); the counteranion could be NO_3^- (**1**, **3**) or ClO_4^- (**2**, **4**), and a monodentate ligand (L, L′) completes the octahedral environment of the manganese ions. For compound **1** L = H_2O and L′ = H_2O or NO_3^-; compound **2** shows two different dinuclear complexes, one of them with L = L′ = H_2O and the other one with L = L′ = ClO_4^-; for compound **3**, L and L′ = H_2O or NO_3^- and for compound **4**, L = H_2O and L′ = ClO_4^-. The characterization by X-ray diffraction shows an important disorder in the crystal for the nitrate compounds, principally for compound **3**, where each monodentate ligand could be a water molecule or a nitrate anion. The antiferromagnetic contribution to the magnetic coupling constant *J* is weaker for the nitrate compounds (**1** and **3**) than for the perchlorate compounds (**2** and **4**), and a ferromagnetic behaviour is found for compound **3**, with $J = +1.4\ cm^{-1}$. The magnetic coupling constant found for compound **1** is $J = -0.5\ cm^{-1}$ and for compounds **2** and **4** it is $-5.6\ cm^{-1}$ and $-3.5\ cm^{-1}$, respectively. Extended Hückel calculations were carried out and there is evidence that the nitrate anions coordinated to the manganese atoms act as π-acid ligands providing a means to diminish the antiferromagnetic contribution.

Introduction

Interest in dinuclear Mn^{III} complexes with a carboxylate ligand is due to their presence in some metalloenzymes such as the Mn-catalase. With the aim of obtaining good model compounds of this enzyme several dinuclear Mn^{III} complexes with the $[Mn_2(\mu\text{-}RCOO)_2(\mu\text{-}O)]^{2+}$ core have been reported in the literature,[1–15] but only 11 of them are characterized by X-ray diffraction and magnetic studies.[5–15]

It is well known that the magnetic interaction for this kind of complex is weak and could be antiferro- or ferromagnetic[16] with *J* values between +18 and –8 cm^{-1}. Three possible distortions of the coordination octahedron can be observed due to the Jahn–Teller effect: (a) compression in the direction of the oxo-bridge, (b) elongation in the direction of one of the blocking ligands or (c) rhombic distortion. In general, compounds with a compressed octahedron in the direction of the oxo-bridging ligand show a ferromagnetic coupling, while complexes with an elongated octahedron (*z*) show antiferromagnetic coupling (Scheme 1). When the distortion is rhombic the magnetic interaction can be ferro- or antiferromagnetic.[5,6,16]

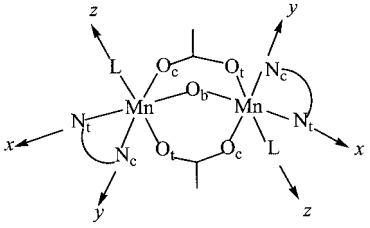

Scheme 1.

Tridentate amines Me_3tacn (*N*,*N*′,*N*′′-trimethyl-1,4,7-triazacyclononane) and tp-tacn (trispyrrolidine-1,4,7-triazacyclononane) favour a compressed octahedron, and a significant ferromagnetic interaction was reported for $[\{Mn(Me_3tacn)\}_2(\mu\text{-}CH_3COO)_2(\mu\text{-}O)](ClO_4)_2$[11,12] ($J = +18.0\ cm^{-1}$) and $[\{Mn(tp\text{-}tacn)\}_2(\mu\text{-}CH_3COO)_2(\mu\text{-}O)](PF_6)_2$[13] ($J = +9.2\ cm^{-1}$). However, tridentate amines TMIP (tris(*N*-methylimidazol-2-yl)phosphane) and HB(pz)$_3$ (hidrotris(1-pyrazolyl)borate) lead to a rhombic distortion, (antiferromagnetic and ferromagnetic contributions are similar) and a small antiferromagnetic interaction was

[a] Departament de Química Inorgànica, Universitat de Barcelona, Martí i Franquès 1–11, 08028 Barcelona, Spain
E-mail: montse.corbella@ub.edu
[b] Departamento de Química Fundamental, Universidade da Coruña,
15071 A Coruña, Spain
[c] Servicios Xerais de Apoio a Investigación, Universidade da Coruña,
15071 A Coruña, Spain

found for compounds $[\{Mn(HBpz_3)\}_2(\mu\text{-}CH_3COO)_2(\mu\text{-}O)]$[14] ($J \approx -1$ cm^{-1}) and $[\{Mn(TMIP)\}_2(\mu\text{-}CH_3COO)_2(\mu\text{-}O)](ClO_4)_2$ ($J \approx -0.4$ cm^{-1}).[15]

When the blocking ligand is bpy (2,2′-bipyridine) the sixth position of the octahedron is occupied by a monodentate ligand; this situation provides a major flexibility to the coordination polyhedron and different types and degrees of distortion can be found. In this work we focused our attention on these kinds of compounds, with the aim of studying the effect of the carboxylate bridge and the monodentate ligand on the magnetic properties. We report here on four new complexes with a general formula $[\{Mn(bpy)L\}(\mu\text{-}RCOO)_2(\mu\text{-}O)\{Mn(bpy)L'\}]^{n+}$ with RCOO = 2-MeC_6H_4COO (**1**, **2**) and 2-FC_6H_4COO (**3**, **4**); the counteranion could be NO_3^- (**1**, **3**) or ClO_4^- (**2**, **4**). A monodentate ligand (L, L′) completes the octahedral environment of the manganese ions and could be H_2O, NO_3^- or ClO_4^-. The coordination of the counteranion to the manganese ion enables us to study the effect of these ligands on the magnetic properties. Extended Hückel calculations were performed with the aim of clarifying the role of these ligands on the magnetic behaviour.

Results and Discussion

Syntheses

The synthetic method used to obtain the dinuclear Mn^{III} complexes is a comproportionation reaction between Mn^{II} and MnO_4^- in the presence of carboxylic acid and a bidentate ligand (2,2′-bipyridine, bpy). The stoichiometry of this reaction is

$$1.6\ MnX_2 + 2\ RCOOH + 0.4\ Bu_4NMnO_4 + 2\ bpy \rightarrow [\{Mn(bpy)L\}(\mu\text{-}RCOO)_2(\mu\text{-}O)\{Mn(bpy)L'\}]X_{2-m} + 0.4\ Bu_4NX + 0.8\ HX + n\ H_2O$$

where RCOOH = 2-MeC_6H_4COOH, 2-FC_6H_4COOH, X = NO_3, ClO_4. These compounds show ionization isomerism, and the monodentate ligand (L and L′) could be H_2O or the counteranion X. When both positions (L and L′) are occupied by X, a neutral complex is obtained ($m = 2$), while if L = H_2O and L′ = X or H_2O the complex is anionic (with $m = 1$ or 0).

The most significant difference between the four compounds synthesized here is their solubility. The perchlorate complexes **2** and **4** are very soluble in MeCN, so it is necessary to add CH_2Cl_2 (for **4**) or CH_2Cl_2 and hexanes (for **2**) to obtain good crystals. In contrast, the nitrate complexes **1** and **3** are less soluble, and subsequently it is necessary to work with dilute solutions to obtain crystalline products. In this case good crystals for X-ray diffraction are obtained directly from the mother liquor.

Infrared spectra of these compounds show two characteristics bands of the carboxylate bridging group at about 1600 and 1380 cm^{-1}. For compounds **1** and **3** the intense band of NO_3^- appears overlapped with the carboxylate one (ca. 1380 cm^{-1}) and it is not possible to distinguish between the coordinated and free ion. Compounds **2** and **4** show three characteristic bands of the ClO_4^- ion at ca. 1100 cm^{-1}. Several weak bands appear in the region between 800–400 cm^{-1} corresponding to the counteranion, the Mn–O–Mn motive and the bpy ligand. The bipyridine ligand shows several bands, some of them in the range 1600–1440 cm^{-1} and 780–635 cm^{-1}.

Description of the Structures

The four compounds reported here display a similar structure. The cationic complex of each compound consists of a dinuclear unit with two carboxylates and one oxo group bridging the two manganese ions. The carboxylate bridging ligand is 2-$MeC_6H_4COO^-$, for **1** and **2**, and 2-$FC_6H_4COO^-$, for **3** and **4**. Each manganese ion is chelated by a bipyridine ligand (bpy), and the coordination sphere can be completed by a molecule of water or by an anion, i.e., nitrate or perchlorate. In all cases the carboxylate group and the aromatic ring of the $RCOO^-$ ligand are not in the same plane. The torsion angle $\delta(O\text{–}C_{carb}\text{–}C_{ar}\text{–}C'_{ar})$ is in the range 15.8–52.4°, however, the compounds with the 2-$FC_6H_4COO^-$ ligand (**3** and **4**) show smaller δ values than the compounds with the 2-$MeC_6H_4COO^-$ ligand (**1** and **2**). The relative orientation of the two coordination octahedrals is quite perpendicular, with the torsion angle τ(L–Mn–Mn–L′) between 84.7–98.1°.

The Mn–O_b distance for the compounds reported here is ca. 1.79 Å, similar to the values found for analogous compounds described in the literature.[5–15] The Mn–O_b–Mn angles for compounds **1**–**4** are between 121° and 125°; these values are also characteristic of these kinds of compounds. An important asymmetry in the carboxylate bridges is observed. In all these compounds, the Mn–O bond length is larger for the carboxylate oxygen atoms *trans* to the monodentate ligand than for the oxygen atoms placed in a *cis* position: d(Mn–O_t) > d(Mn–O_c). The bond lengths d(Mn–O_t) (ca. 2.16 Å) and d(Mn–O_N) (ca. 2.17 Å) are similar, while the distances d(Mn–O_W) and d(Mn–O_{Cl}) are longer (ca. 2.27 Å and ca. 2.36 Å, respectively). [O_N, O_W and O_{Cl} correspond to the oxygen atom of the L ligand coordinated to the manganese ions: nitrate, water and perchlorate, respectively.] Therefore, the monodentate ligand in these kinds of complexes produces an important effect on the coordination polyhedra of the manganese ions.

[{Mn(bpy)(H_2O)}(μ-2-MeC_6H_4COO)$_2$(μ-O){Mn(NO_3)(bpy)}]NO_3·2CH_3CN·2H_2O (1)

This compound shows a certain disorder in the crystal structure between one water molecule and one nitrate anion. The labile position in Mn(2) is always occupied by a water ligand, O(1s). However, in Mn(1) only in 57% of the cases is this position occupied by a water ligand, O(5s), while in the rest of the cases it is occupied by one nitrate anion, O(6). In Figure 1 it is possible to see both ligands near to Mn(1), although only one of them is present in each dinuclear unit. The most relevant distances and angles are listed in Table 1. The nitrate ligand is situated approxi-

Table 1. Selected interatomic distances [Å] and angles [°] for compound [{Mn(bpy)(H_2O)}(μ-2-$CH_3C_6H_4COO$)$_2$(μ-O){Mn(NO_3)-(bpy)}](NO_3)·2CH_3CN·2H_2O (**1**) with estimated standard deviations (Esd's) in parentheses.

Mn(1)–O(1)	1.796(3)	Mn(2)–O(1)	1.784(2)
Mn(1)–O(2)	1.959(3)	Mn(2)–O(5)	1.958(3)
Mn(1)–N(1)	2.075(3)	Mn(2)–N(3)	2.069(3)
Mn(1)–N(2)	2.076(3)	Mn(2)–N(4)	2.083(3)
Mn(1)–O(4)	2.151(3)	Mn(2)–O(3)	2.123(3)
Mn(1)–O(6)	2.258(3)	Mn(2)–O(1s)	2.211(3)
Mn(1)–Mn(2)	3.1480(7)	Mn(1)–O(1)–Mn(2)	123.13(14)
O(6)–Mn(1)–Mn(2)–O(1s)	97.20(13)		
O(3)–C(11)–C(12)–C(17)	–15.78(60)		
O(4)–C(18)–C(19)–C(24)	41.83(59)		
O(7)–N(5)–O(6)–Mn(1)	–101.27(82)		
O(8)–N(5)–O(6)–Mn(1)	79.21(78)		

mately perpendicular to the *z* axis, (defined in the L ligand direction as indicated above) with γ(O–*N*–O–Mn) angles of ca. 98°.

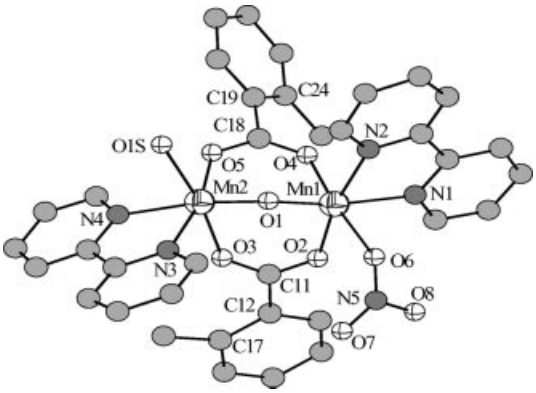

Figure 1. Drawing of the cation [{Mn(bpy)(H_2O)}(μ-2-$CH_3C_6H_4COO$)$_2$(μ-O){Mn(NO_3)(bpy)}]$^+$ in compound **1** showing two ligands coordinated in the same position for Mn(1): nitrate and water, corresponding to the two forms of the dinuclear unit present in the crystal.

There are hydrogen bonds between the nitrate anions and the coordinated water molecule generating a one-dimensional system. On one side, two Mn(2) ions of different dinuclear entities are bridged through the ionic nitrate anions and the coordinated water ligand, Mn(2)–O(1s)···O(10)–N–O(11)···O(1s)–Mn(2). On the other side, two Mn(1) ions of neighbour dinuclear complexes are bridged through the nitrate ion coordinated to one Mn(1) ion and the water molecule coordinated to the other Mn(1) ion, Mn(1)–O(6)–N–O(7)···O(5s)–Mn(1) (Figure 2).

[{Mn(bpy)(H_2O)}$_2$(μ-2-MeC_6H_4COO)$_2$(μ-O)]-[{Mn(ClO_4)(bpy)}$_2$(μ-2-MeC_6H_4COO)$_2$(μ-O)](ClO_4)$_2$·CH_2Cl_2 (2)

The crystal structure of this compound shows two different dinuclear complexes. One of them is cationic, with the labile position on each manganese occupied by one water molecule, and the other one is neutral, with a perchlorate coordinated to each manganese in the labile position. Figure 3 shows the two dinuclear entities and the most important distances and angles are reported in Table 2. The cationic and neutral dinuclear complexes are bridged through hydrogen bonds between the water ligand of one entity and the perchlorate ligand of the other: Mn(3)–O_W···O_{Cl}–Mn(2). The same water ligand is also hydrogen bonded to one of the perchlorate anions.

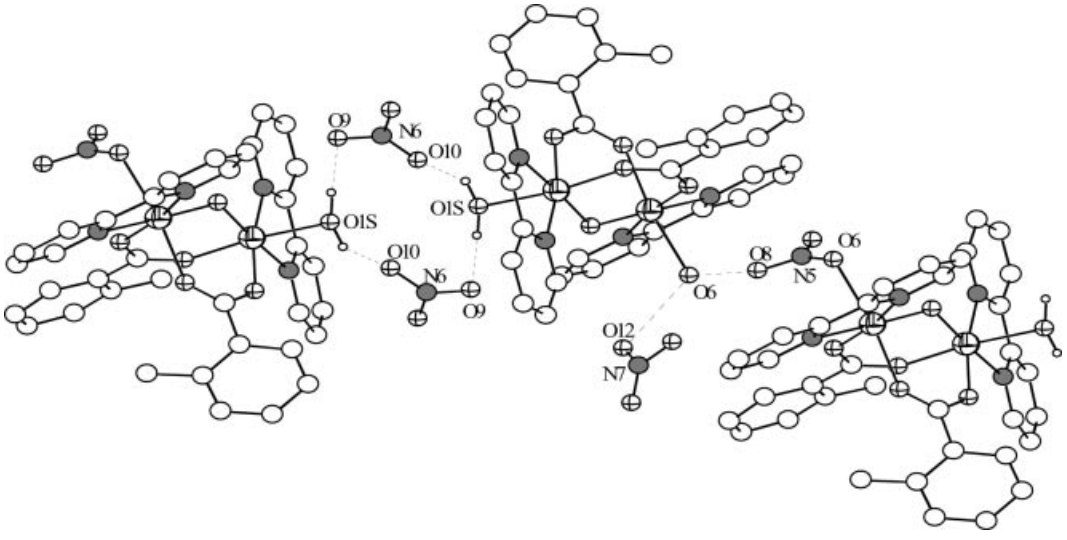

Figure 2. Plot of the hydrogen bonds present in the crystal of compound **1** between the nitrate ions and the water ligand on Mn(2), and between the nitrate ligand and water ligand on Mn(1).

Table 2. Selected interatomic distances [Å] and angles [°] for compound $[\{Mn(bpy)(H_2O)\}_2(\mu\text{-}2\text{-}CH_3C_6H_4COO)_2(\mu\text{-}O)][\{Mn(ClO_4)(bpy)\}_2(\mu\text{-}2\text{-}CH_3C_6H_4COO)_2(\mu\text{-}O)](ClO_4)_2\cdot 0.5CH_2Cl_2$ (**2**).

Mn(1)–O(1)	1.787(4)	Mn(3)–O(14)	1.805(6)
Mn(1)–O(2)	1.933(4)	Mn(3)–O(15)	1.962(5)
Mn(1)–N(1)	2.049(5)	Mn(3)–N(5)	2.060(6)
Mn(1)–N(2)	2.050(5)	Mn(3)–N(6)	2.072(6)
Mn(1)–O(4)	2.160(4)	Mn(3)–O(17)	2.145(6)
Mn(1)–O(6)	2.410(4)	Mn(3)–O(19)	2.214(7)
Mn(2)–O(1)	1.783(4)	Mn(4)–O(14)	1.780(5)
Mn(2)–O(5)	1.916(5)	Mn(4)–O(18)	1.959(5)
Mn(2)–N(3)	2.032(5)	Mn(4)–N(7)	2.072(5)
Mn(2)–N(4)	2.051(5)	Mn(4)–N(8)	2.087(6)
Mn(2)–O(3)	2.131(4)	Mn(4)–O(16)	2.152(4)
Mn(2)–O(10)	2.407(4)	Mn(4)–O(20)	2.246(6)
Mn(1)–Mn(2)	3.1182(13)	Mn(3)–Mn(4)	3.149(3)
Mn(1)–O(1)–Mn(2)	121.66(22)	Mn(3)–O(14)–Mn(4)	122.90(28)
O(6)–Mn(1)–Mn(2)–O(10)	112.15(13)	O(19)–Mn(3)–Mn(4)–O(20)	–90.00(21)
O(3)–C(1)–C(2)–C(3)	52.39(94)	O(16)–C(37)–C(38)–C(39)	45.75(97)
O(4)–C(9)–C(10)–C(11)	–45.97(95)	O(17)–C(45)–C(46)–C(47)	–43.32(96)

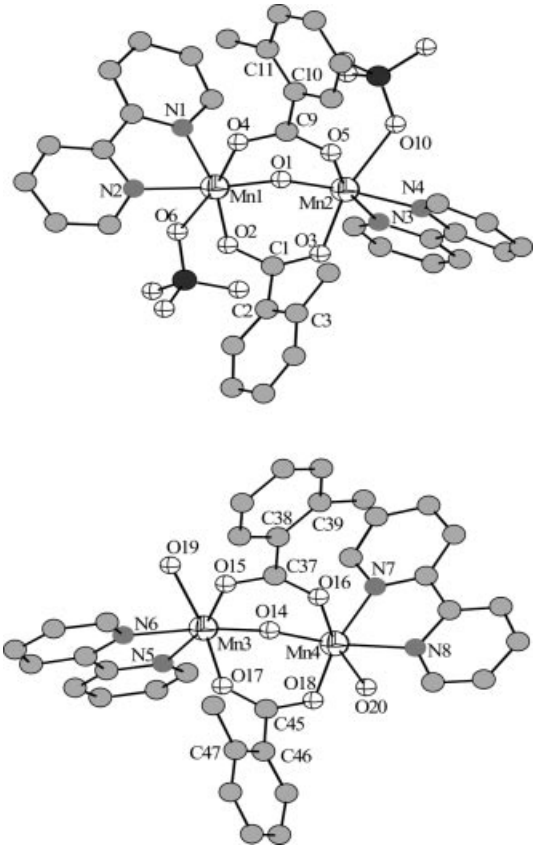

Figure 3. Drawing of the dinuclear complexes $[\{Mn(bpy)(H_2O)\}_2(\mu\text{-}2\text{-}CH_3C_6H_4COO)_2(\mu\text{-}O)]^{2+}$ (bottom) and $[\{Mn(ClO_4)(bpy)\}_2(\mu\text{-}2\text{-}CH_3C_6H_4COO)_2(\mu\text{-}O)]$ (top) present in the crystal of compound **2**.

[{Mn(bpy)(H$_2$O)}(μ-2-FC$_6$H$_4$COO)$_2$(μ-O){Mn(NO$_3$)(bpy)}]NO$_3$·H$_2$O (3)

Similarly to compound **1**, a certain delocalization between the water and nitrate ligands is observed. In this case both manganese ions show disorder: in 31% of the dinuclear complexes both manganese ions present a coordinated water molecule, another 20% have one nitrate anion coordinated to each manganese and the last 49% show an asymmetric coordination (in one manganese ion the monodentate ligand is a nitrate ion, while in the other one it is a water molecule). Figure 4 shows the dinuclear complex with both possible ligands in the labile position. In comparison to compound **1**, the orientation of the nitrate ligand is different; in this case the ligand is placed quite parallel to the *z* axis, with γ(O–N–O–Mn) angles of ca. 20°. Selected interatomic bond lengths and angles are listed in Table 3. This compound shows disorder in the position of the F atoms of the carboxylate bridges: F(1) bonded to C(17) and F(1′) bonded to C(13) with an occupancy of 86% and 14%, respectively. And for the other carboxylate there is F(2) bonded to C(24) and F(2′) bonded to C(20) with an occupancy of 82% and 18%, respectively. Mn(1) and Mn(2) of neighbour complexes are bridged by hydrogen bonds between a water ligand of one dinuclear complex and a nitrate ligand of another complex, generating a 1D system.

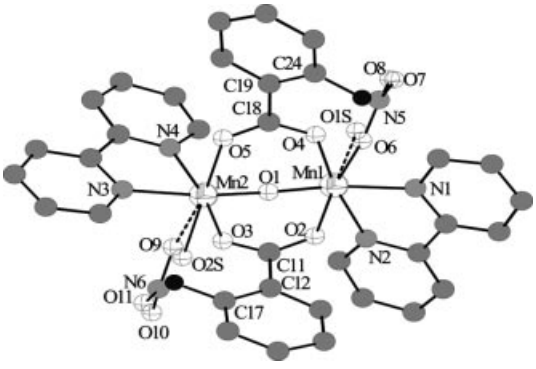

Figure 4. Drawing of the dinuclear complex of compound **3**. In the crystal the monodentate ligand attached to each manganese atom could be either nitrate or water. In the picture, both ligands are shown in each position.

[{Mn(bpy)(H$_2$O)}(μ-2-FC$_6$H$_4$COO)$_2$(μ-O){Mn(ClO$_4$)(bpy)}]ClO$_4$·2CH$_2$Cl$_2$ (4)

Figure 5 show the dinuclear cationic complex of compound **4**. In this compound the labile position is occupied by one water ligand in Mn(1) and one perchlorate anion in

Table 3. Selected interatomic distances [Å] and angles [°] for compound [{Mn(bpy)(H_2O)}(μ-2-FC_6H_4COO)$_2$(μ-O){Mn(NO_3)(bpy)}]-NO_3·H_2O (**3**).

Mn(1)–O(1)	1.791(3)	Mn(2)–O(1)	1.791(3)
Mn(1)–O(4)	1.987(3)	Mn(2)–O(3)	1.986(3)
Mn(1)–N(2)	2.075(3)	Mn(2)–N(3)	2.087(4)
Mn(1)–N(1)	2.081(4)	Mn(2)–N(4)	2.087(3)
Mn(1)–O(6)	2.15(2)	Mn(2)–O(9)	2.14(3)
Mn(1)–O(2)	2.187(3)	Mn(2)–O(5)	2.187(3)
Mn(1)–O(1S)	2.33(2)	Mn(2)–O(2S)	2.34(3)
Mn(1)–Mn(2)	3.179(13)	Mn(1)–O(1)–Mn(2)	125.08(17)
O(1S)–Mn(1)–Mn(2)–O(9)	89.6(11)		
O(1S)–Mn(1)–Mn(2)–O(2S)	93.6(10)		
O(6)–Mn(1)–Mn(2)–O(2S)	88.8(10)		
O(6)–Mn(1)–Mn(2)–O(9)	84.7(11)		
O(4)–C(18)–C(19)–C(24)	–23.4(6)		
O(3)–C(11)–C(12)–C(17)	–16.2(6)		
O(7)–N(5)–O(6)–Mn(1)	–174.5(14)		
O(8)–N(5)–O(6)–Mn(1)	16.3(27)		
O(10)–N(6)–O(9)–Mn(2)	–165.8(22)		
O(11)–N(6)–O(9)–Mn(2)	23.0(39)		

Mn(2). Selected interatomic bond lengths and angles are listed in Table 4. The water ligand bonds, through hydrogen atoms, the ionic perchlorate and the perchlorate ligand of the neighbour dinuclear entity. These bonds create a one-dimensional system depicted in Figure 6.

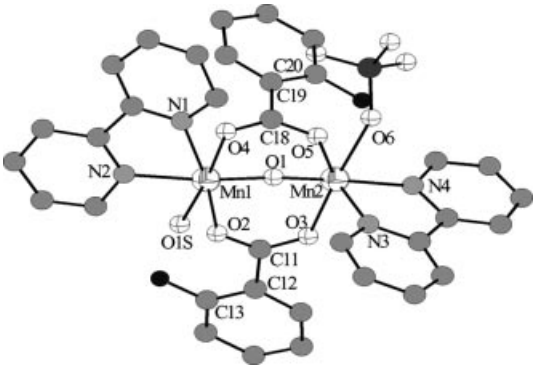

Figure 5. Drawing of the cationic complex [{Mn(bpy)(H_2O)}(μ-2-FC_6H_4COO)$_2$(μ-O){Mn(ClO_4)(bpy)}]$^+$ of compound **4**.

Table 4. Selected interatomic distances [Å] and angles [°] for compound [{Mn(bpy)(H_2O)}(μ-2-FC_6H_4COO)$_2$(μ-O){Mn(ClO_4)(bpy)}]-ClO_4·$2CH_2Cl_2$ (**4**).

Mn(1)–O(1)	1.787(6)	Mn(2)–O(1)	1.778(5)
Mn(1)–O(2)	1.978(5)	Mn(2)–O(5)	1.949(7)
Mn(1)–N(1)	2.070(6)	Mn(2)–N(3)	2.037(8)
Mn(1)–N(2)	2.068(9)	Mn(2)–N(4)	2.031(8)
Mn(1)–O(4)	2.185(6)	Mn(2)–O(3)	2.142(5)
Mn(1)–O(1S)	2.204(6)	Mn(2)–O(6)	2.312(5)
Mn(1)–Mn(2)	3.1543(19)		
Mn(1)–O(1)–Mn(2)	124.4(3)		
O(1s)–Mn(1)–Mn(2)–O(6)	–93.6(2)		
O(5)–C(18)–C(19)–C(20)	19.9(11)		
O(2)–C(11)–C(12)–C(13)	19.1(12)		

Compounds **1**–**4** show intramolecular hydrogen bonds between the groups (or atoms) in the *ortho* position on the aromatic ring, the oxygen atoms of the carboxylate groups and the hydrogen atom of the bpy ligand (Figure 7). In compounds **3** and **4** the fluorine atom on the aromatic ring shows a preference for the position closest to the O_c atom and the hydrogen bonds present in these compounds are F···H_{bpy}, H_{Ph}···O_t and O_c···H_{bpy}. In contrast, the methyl group on the aromatic ring is placed closest to the O_t atom

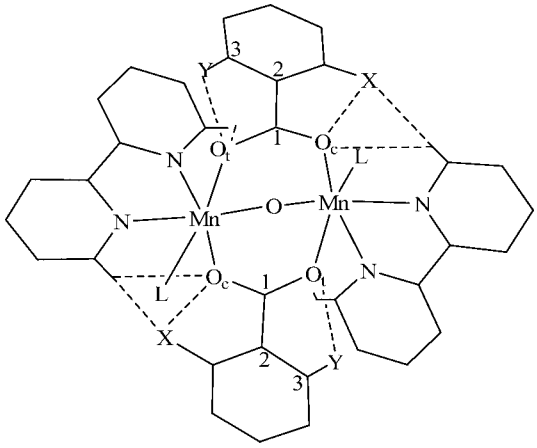

Figure 7. Drawing depicting the intramolecular H bonds presents in the dinuclear complexes. For compounds **1** and **2**, X = H_{Ph} and Y = Me, and for compounds **3** and **4**, X = F and Y = H_{Ph}.

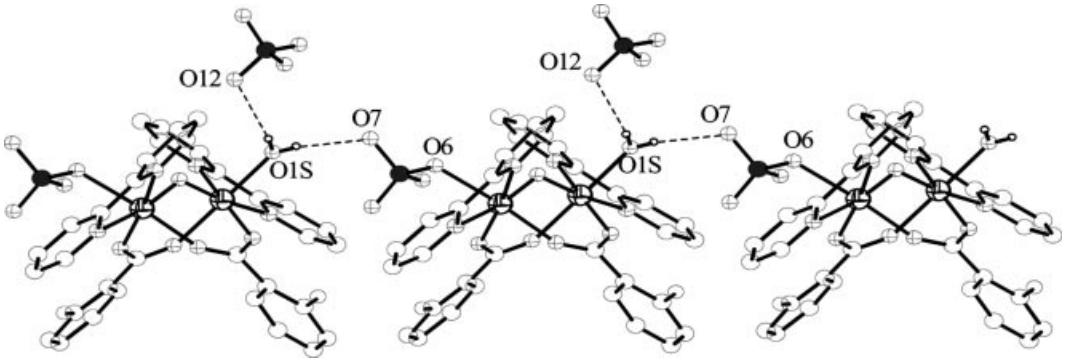

Figure 6. Plot of the hydrogen bonds present in the crystal of compound **4** between the coordinated perchlorate anion and the water ligand, giving a one-dimensional system, and between the water ligand and the ionic perchlorate.

and in these cases the observed hydrogen bonds are $H_{Ph}\cdots O_c$, $O_c\cdots H_{bpy}$ and $O_t\cdots H_{Me}$, and these bonds are weaker than in the fluoro complexes (Table 5).

Table 5. Intramolecular hydrogen bonds and torsion angles, $\delta(O_tC_1C_2C_3)$ and τ(LMnMnL).

	$O_c\cdots H_{Ph}$ [Å]	$O_c\cdots H_{bpy}$ [Å]	$O_t\cdots H_{Me}$ [Å]	δ [°]	τ [°]
1	2.43/2.57	2.48/2.45	2.45/2.63	15.8/–41.7	97.3
2 (ClO_4)	2.77/2.63	2.38/2.45	2.72/2.64	52.4/–46.1	97.8
2 (H_2O)	2.64/2.65	2.55/2.43	2.66/2.52	45.8/–43.4	89.6
	$O_c\cdots H_{bpy}$	$F\cdots H_{bpy}$	$O_t\cdots H_{Ph}$		
3	2.54/2.55	2.37/2.34	2.51/2.49	–21.6/–15.6	89.1
4	2.47/2.54	2.24/2.32	2.43/2.38	16.0/11.7	93.6

Magnetic Properties

Magnetic susceptibility data were recorded for all complexes from room temperature to 4 K (or 2 K for **1** and **3**). The $\chi_M T$ product is ca. 5.6–5.9 $cm^3 mol^{-1}$ K at room temperature, which is close to the expected value for two uncoupled Mn^{III} ions (6.0 $cm^3 mol^{-1}$ K). For compounds **1**, **2** and **4**, the $\chi_M T$ decreases with the temperature (very slowly for compound **1**) reaching a value of 0.4–0.8 $cm^3 mol^{-1}$ K at 4 K for compounds **2** and **4** and 4.4 $cm^3 mol^{-1}$ K for compound **1** (Figure 8). This behaviour is typical of an antiferromagnetic coupling between two Mn^{III} ions. In contrast, for compound **3**, the $\chi_M T$ values increase when the temperature descends, reaching a maximum value of 6.43 $cm^3 mol^{-1}$ K at 16.5 K; at lower temperatures $\chi_M T$ decreases until 4.94 $cm^3 mol^{-1}$ K at 2 K. This behaviour is characteristic of ferromagnetic coupling. The expected value of $\chi_M T$ for a system with a ground state $S = 4$ must be 10 $cm^3 mol^{-1}$ K; the lower value found at 16.5 K and a decreasing of $\chi_M T$ below this temperature could be explained by the presence of zero-field splitting in the ground state and/or the intermolecular interactions. Magnetization measurements at 2 K, for compound **3**, show a $M/N\beta$ value of 5.5 at 50000 G, in agreement with the weak ferromagnetic interaction. For compounds **2** and **4** the χ_M vs. T plot (Figure 8, inset) shows a maximum at 16.8 K (χ_M = 0.11 $cm^3 mol^{-1}$) and at 10.2 K (χ_M = 0.18 $cm^3 mol^{-1}$), respectively, indicating a major antiferromagnetic coupling for the former compound.

The spin Hamiltonian $H = -J\, S_1 \cdot S_2$ was used to fit the experimental data assuming that the two Mn^{III} ions present the same g value. The parameters J and g obtained from a least-squares fitting of the χ_M vs. T data to the theoretical equation are listed below. Similar results are obtained by fitting the $\chi_M T$ vs. T data. For the ferromagnetic compound (**3**), the theoretical equation was modified including the parameter of axial zero-field splitting, D, in the ground state $S = 4$. The Hamiltonian describing the ZFS was: $H_D = D[S_z^2 - S(S+1)/3]$. The best fits correspond to: $J = -0.5$ cm^{-1} and $g = 1.98$, with $R = 5.5 \times 10^{-5}$ for **1**; $J = -5.6$ cm^{-1} and $g = 1.98$, with $R = 4.1 \times 10^{-4}$ for **2**; $J = +1.4$ cm^{-1}, $|D| = 0.4$ cm^{-1} and $g = 1.98$, with $R = 5.8 \times 10^{-5}$ for **3** and $J = -3.5$ cm^{-1} and $g = 1.98$, with $R = 2.6 \times 10^{-5}$ for **4**.

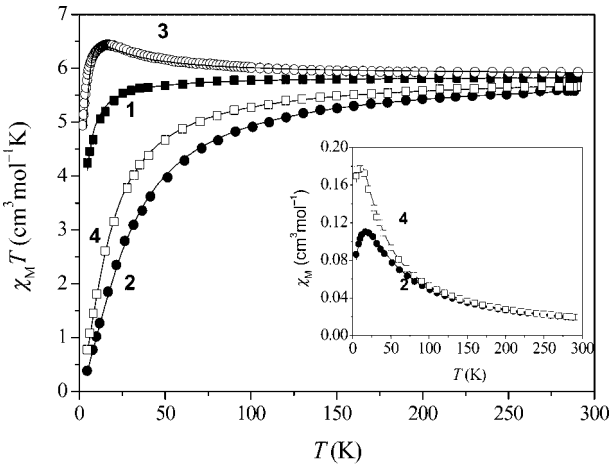

Figure 8. $\chi_M T$ vs. temperature plot for compounds **1**–**4**. The inset is the χ_M vs. T plot for compounds with a perchlorate anion (**2** and **4**). The solid line is the best fit of the experimental data.

The four compounds show a moderate magnetic coupling. The strongest antiferromagnetic coupling was found for compound **2** while a ferromagnetic coupling was observed for compound **3**. As indicated in the previous section, in all cases the counteranion could be coordinated to the manganese ions. For compounds **2** and **4** the perchlorate anion is coordinated in 50% of the manganese ions, while for compounds **1** and **3**, the coordination of the nitrate anion is lower: only ca. 21% of the manganese ions show a nitrate ligand for compound **1**, while for compound **3** ca. 45% of the manganese ions show a coordinated nitrate anion. A comparison of the magnetic coupling constant of the four compounds indicates that, with the same carboxylate bridges, the perchlorate complexes show greater antiferromagnetic coupling than the nitrate complexes, with a difference of ca. 5 cm^{-1}. On the other hand, with the same anion, complexes with 2-MeC_6H_4COO bridges show a stronger antiferromagnetic interaction than do complexes with 2-FC_6H_4COO bridges, with a difference of ca. 2 cm^{-1}. The magnitude of the magnetic exchange interaction between the two Mn^{III} ions found in compounds **1**–**4** may be compared with those reported for other dinuclear Mn^{III} complexes with the general formula $[\{Mn(bpy)L\}_2(\mu\text{-}RCOO)_2(\mu\text{-}O)]^{n+}$ ($n = 2$ for neutral L ligands and $n = 0$ for anionic L ligands). Table 6 summarizes the most important structural parameters and the magnetic coupling constants for these compounds. As an example, the $Mn\text{–}O_b\text{–}Mn$ angle is in the range 122–125° and the $Mn\text{–}O_b$ distances are very similar for all compounds, since the d-orbital pointing to the oxo bridge is empty the magnitude of the magnetic interaction will not be very sensitive to this parameter.

Considering the x axis in the oxo-bridge direction and the z axis in the L direction (Scheme 1) we can find approximate values of the octahedron axes lengths by the addition of the Mn–ligand distances: $d(Mn\text{–}O_b) + d(Mn\text{–}N_t)$ (x axis), $d(Mn\text{–}O_c) + d(Mn\text{–}N_c)$ (y axis) and $d(Mn\text{–}L) + d(Mn\text{–}O_t)$ (z axis). When the distance values for the x and y axis are similar, and smaller than the distance value found for the z axis [$d(O_b\cdots N_t) \approx d(O_c\cdots N_c) < d(L\cdots O_t)$], the coordination

Table 6. Magnetic coupling constants[a] and selected structural parameters for $[\{Mn(bpy)L\}_2(\mu\text{-}RCOO)_2(\mu\text{-}O)]^{n+}$ complexes with the 2,2′-bipyridine (bpy) and monodentate L ligand as blocking ligands.[b]

	L	Mn–O–Mn α [°]	Mn–O_b [Å]	Mn–O_c [Å]	Mn–O_t [Å]	Mn–L [Å]	x[c] [Å]	y[c] [Å]	z[c] [Å]	γ[d] [°]	J [cm^{-1}]
1	H_2O H_2O/NO_3	123.1	1.79	1.96	2.14	2.23	3.86	4.04	4.37	98	–0.5
2	H_2O ClO_4	122.3	1.79	1.94	2.15	2.32	3.86	3.99	4.47		–5.6
3	H_2O NO_3	125.1	1.79	1.99	2.19	2.24	3.87	4.07	4.43	20	+1.4
4	H_2O ClO_4	124.4	1.78	1.96	2.16	2.26	3.83	4.01	4.42		–3.5
5	OH NO_3	124.1	1.78	1.97	2.16	2.21	3.85	4.05	4.37	177	+2.0
6	N_3	122.0	1.80	2.04	2.13	2.12	3.89	4.19	4.25		+17.6
7	H_2O	124.7	1.79	1.95	2.19	2.25	3.85	4.01	4.44		–2.9
8	H_2O	124.6	1.79	1.96	2.24	2.20	3.86	4.02	4.44		–0.7
9	H_2O	122.9	1.78	1.94	2.16	2.31	3.85	3.99	4.47		–6.8
10	Cl	124.3	1.78	1.94	2.20	2.56	3.87	4.01	4.76		–8.2
11	H_2O	125.2	1.77	2.00	2.17	2.21	3.85	4.06	4.38		+4.7
11	H_2O NO_3	121.8	1.81	1.93	2.13	2.25	3.84	3.98	4.38	114	+4.7

[a] Values using the $H = -J\ S_1 \cdot S_2$ convention. [b] See Scheme 1 for the terminology O_c, O_b, N_t and N_c. [c] x, y and z symbolize the distances between ligands in the *trans* position, e.g., $x = O_b \cdots N_t$ is the addition of both manganese–ligand distances, $d(O_b \cdots N_t) = d(Mn\text{–}O_b) + d(Mn\text{–}N_t)$, $y = d(O_c \cdots N_c)$ and $z = d(O_t \cdots L)$. [d] γ = ONOMn angle. All distances and angle values are the average of the two manganese centres, and for **2** it is also the average for the two complexes present in the crystal. **5** = $[\{Mn(OH)(bpy)\}(\mu\text{-}PhCOO)_2(\mu\text{-}O)\{Mn(NO_3)(bpy)\}]$;[5] **6** = $[\{Mn(N_3)(bpy)\}_2(\mu\text{-}PhCOO)_2(\mu\text{-}O)]$;[6] **7** = $[\{Mn(bpy)(H_2O)\}_2(\mu\text{-}ClCH_2COO)_2(\mu\text{-}O)](ClO_4)_2$;[8] **8** = $[\{Mn(bpy)(H_2O)\}_2(\mu\text{-}ClCH_2COO)_2(\mu\text{-}O)](NO_3)_2$.[8] **9** = $[\{Mn(bpy)(H_2O)\}_2(\mu\text{-}CH_3COO)_2(\mu\text{-}O)](PF_6)_2$;[9] **10** = $[\{Mn(Cl)(bpy)\}_2(\mu\text{-}CH_3COO)_2(\mu\text{-}O)]$;[6] **11** = $[\{Mn(bpy)(H_2O)\}_2(\mu\text{-phtha})_2(\mu\text{-}O)]$ $[\{Mn(bpy)(H_2O)\}(\mu\text{-phtha})_2(\mu\text{-}O\{Mn(bpy)(NO_3)\}](NO_3)_3$ (phtha = phthalate).[10]

polyhedron is considered elongated, while if the distance for the x axis is shorter than the distances for the z and y axis $[d(O_b \cdots N_t) < d(O_c \cdots N_c) \approx d(L \cdots O_t)]$, the octahedron is compressed. Finally, if the distances of the three axes are different the octahedron presents a rhombic distortion. Then, we can define the distortion parameter as $(z - y)/(y - x)$, where $z = d(L \cdots O_t)$, $y = d(O_c \cdots N_c)$ and $x = d(O_b \cdots N_t)$, and the greater values of this parameter correspond to the compounds with a major antiferromagnetic coupling. For the four compounds reported here the major distortion parameter value corresponds to the complexes with perchlorate as the monodentate ligand. Figure 9 shows the distortion parameter for the compounds reported in Table 6, in front of the magnetic coupling constant. The two extreme values of the distortion parameter are found for compound **6**, with a distortion parameter close to zero, and for compound **10**, with a distortion parameter of 5.36.

Only one of the compounds collected in Table 6 shows compressed octahedra; this is the case for compound **6** $[\{Mn(N_3)(bpy)\}_2(\mu\text{-}C_6H_4COO)_2(\mu\text{-}O)]$.[6,7] As in the case of the complexes with tridentate amines[11–13] a ferromagnetic interaction is also observed for this compound. Compound **10** $[\{MnCl(bpy)\}_2(\mu\text{-}CH_3COO)_2(\mu\text{-}O)]$[7] is the compound with the most elongated octahedra and shows major antiferromagnetic coupling. The other compounds show closest distortion parameters between 1.5 and 3.5. Two compounds reported here, **2** and **4**, in which the perchlorate anion is coordinated to the manganese ions, also show elongated octahedra, and in general the magnitude of the antiferromagnetic coupling agrees with the values found for compounds **9**[9] and **10**.[7]

When the nitrate anion is coordinated to the manganese ion the Mn–L distances are shorter. Consequently, the elongation in the z axis is moderate, and the distortion is intermediate between elongated and rhombic. The first

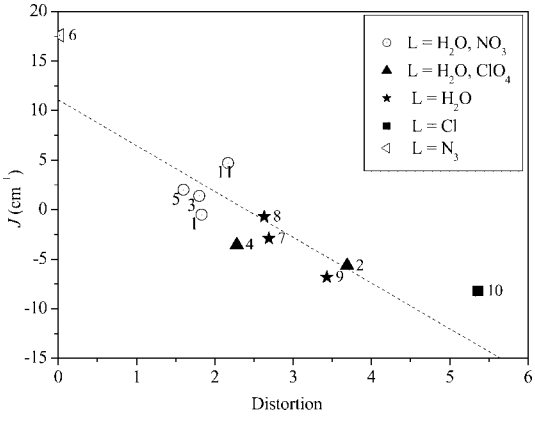

Figure 9. Correlation between the distortion around the Mn^{III} ions and the magnetic interaction. The degree of distortion was measured as $(z - y)/(y - x)$, where $z = d(L \cdots O_t)$, $y = d(O_c \cdots N_c)$ and $x = d(O_b \cdots N_t)$ (See Scheme 1). The dashed line is the plot of the function $J = 11.1 - (4.6 \times \text{distortion})$, and the symbols are the experimental data.

compound of this kind described in the literature, $[\{Mn(OH)(bpy)\}(\mu\text{-}C_6H_4COO)_2(\mu\text{-}O\{Mn(NO_3)(bpy)\}]$ (**5**),[5] presents a rhombic distortion, and a ferromagnetic interaction was found. Compound **3** also shows a ferromagnetic coupling, while compound **1** is weakly antiferromagnetic. Another analogous compound reported in the literature has two different dinuclear complexes in the crystal, $[\{Mn(bpy)(H_2O)\}_2(\mu\text{-phtha})_2(\mu\text{-}O)][\{Mn(bpy)(H_2O)\}(\mu\text{-phtha})_2(\mu\text{-}O)\{Mn(bpy)(NO_3)\}](NO_3)_3$ (**11**) (phtha = phthalate),[10] one of them with two water molecules and the other with one water and one nitrate ligand. A net ferromagnetic interaction was reported for this compound, where we could expect a different degree of magnetic interaction in each dinuclear complex.

For dinuclear Mn^{III} compounds with four electrons in each manganese ion (i and j) the magnetic coupling constant is $J = 1/16\ \Sigma\ J_{ij}$.[17] Because of the presence of one empty orbital in each manganese ion there are eight crossing interactions between each single occupied orbital and the empty orbital (x^2–y^2), and this kind of interaction is postulated as ferromagnetic.[17] The most important antiferromagnetic contribution to the magnetic behaviour is due to the $xz(1)/xy(2)$ interaction (Figure 10). The other π^* interaction through the oxo-bridging ligand, the $xy(1)/xz(2)$ interaction, could be sensitive to the Mn–O_b–Mn angle. For these kinds of complexes, with $\alpha \approx 124°$, an antiferromagnetic interaction can be expected. The same occurs with the $z^2(1)/z^2(2)$ interaction: for Mn–O_b–Mn angles far from 90° an antiferromagnetic interaction can be expected. Other antiferromagnetic contributions are the $z^2(1)/xz(2)$ and the $xy(1)/z^2(2)$ interactions. Subsequently, there are an important number of interactions of both signs, ferro- and antiferromagnetic, and the resultant magnetic behaviour of a compound is because of the balance of these contributions.

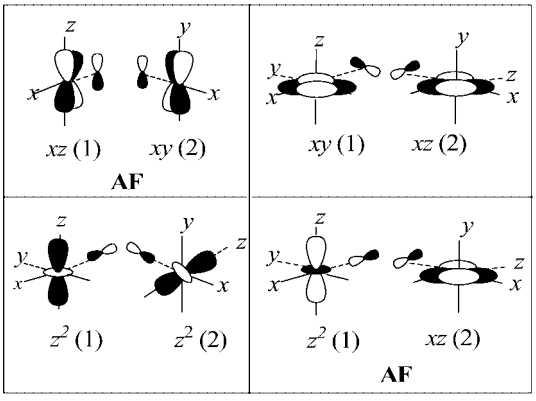

Figure 10. Schematic representation of the magnetic exchange pathway.

Extended Hückel Calculations

In an attempt to rationalize the magnetic properties of the compounds **1**–**4**, we found that their molecular geometries can be differentiated by the following factors:

(a) the nature of the substituent of the benzoate bridge, with a CH_3 group for compounds **1** and **2** and an electron-withdrawing F atom for compounds **3** and **4**;

(b) the position of the F atom or the CH_3 group in the aromatic ring: the CH_3 group is on the side of the O_t atom, while the F atom is placed on the side of the O_c atom; (Figure 7)

(c) the nature of the monodentate ligand, which could be H_2O, NO_3 or ClO_4;

(d) the dihedral angle between the carboxylate group and the phenylic ring, defined by the $\delta(O_tC_1C_2C_3)$ angle (Figure 7);

(e) the relative orientation of the nitrate ligand in the environment of manganese, defined by the γ(ONOMn) angle.

With the aim of determining the effect of these factors on the magnetic properties, Extended Hückel calculations were carried out on the crystallographic coordinates of compounds **1**–**4** using the CACAO program.[18] Taking into consideration that in compounds **1** and **3** the monodentate ligand H_2O could be replaced by the NO_3 anion, the different complexes present in the crystal, in each case, have been studied. Other calculations carried out were:

– the dihedral angle between the COO group and the aromatic ring, δ, was modified from the original crystallographic coordinates and two values are considered: $\delta = 17°$ and 45°;

– the substituent on the aromatic ring, CH_3 or F was replaced by the other group (F or CH_3, respectively), in the same position as the original compound, and also, in the opposite position;

– for compounds **1** and **3** the crystallographic coordinates of the nitrate group have been modified, with γ angles between 0–180°;

– with the aim of making comparisons with other compounds with nitrate ligands calculations with the crystallographic coordinates of compounds **5**[5] and **11**[10] have been also carried out. And the position of the nitrate ligand was also modified with γ angles between 0–180°.

Considering the axis depicted in Scheme 1, the x^2–y^2 orbital of each manganese atom points to the O_b, O_c of the carboxylate group and both N atoms of the bidentate ligand, and the z^2 orbital points to the monodentate ligand L and the O_t atom. The energy diagram and the shape of the MO's are similar for all the studied compounds except for the MO with contributions from the z^2 orbital of the manganese ions. In all cases, the z^2 orbitals of the manganese ions contribute significantly to the first single occupied orbitals. The z^2 orbital of each manganese ion could overlap with the orbitals of the ligands in the z axis (L and O_t), and to a lesser degree with the ligands in the equatorial plane (O_b, N_t, N_c and O_c). The two resultant molecular orbitals are each considerably localized on one of the manganese atoms, even if a small contribution of the bridging ligands is present.

The analysis of the results shows a very small effect in the energy and composition of the MO by modification of the torsion angle between the carboxylate group and the aromatic ring, and the last with its substituent group. However, both factors modify the positive charge on the manganese ions. The clearest effect is due to the substituent in the aromatic ring: with the same crystallographic parameters the exchange CH_3/F slightly modifies the positive charge on the manganese ions (the methyl group, with a donor effect, decreases the positive charge on the manganese ions while the F atom, with a withdrawing effect, increases the positive charge).

The dinuclear complexes listed in Table 6 show different kinds of monodentate ligands: H_2O, OH^-, ClO_4^-, Cl^-, NO_3^- and N_3^-. The H_2O, ClO_4^- and Cl^- ligands act as σ-donor ligands, and their HOMO's are low in energy. On the other hand, the NO_3^- and N_3^- ligands show two orbitals with similar energies to the d-orbitals of the manganese ions: a

filled nonbonding orbital with a σ-donor character and an empty π* orbital.

For the nitrate complexes with 2-MeC_6H_4COO (**1**), 2-FC_6H_4COO (**3**) and 2-$OOCC_6H_4COO$ (**11**) an important overlap between the empty π* orbital of the nitrate ligand and the z^2 of the Mn^{III} ion is observed. Then, two molecular orbitals $\pi_L^* \pm z^2_{Mn}$ were found for each metallic centre. In contrast, for compound **5** [{Mn(OH)(bpy)}(μ-PhCOO)$_2$-(μ-O){Mn(NO_3)(bpy)}][5] no contribution of the π* orbital of the nitrate ligand was found in the z^2 orbital. For this compound the nitrate ligand acts only as a σ-donor ligand. The energy of the π_L^* orbital is very sensitive to the distortions in the nitrate anion. For compound **5**, the N–O distances are quite a bit shorter than those for complexes **1**, **3** and **11** (average of 1.19 Å for **5** and average of 1.25 Å for **1**, **3** and **11**) therefore the π_L^* was found at a higher energy and no appreciable interaction with the z^2 of the metal was observed.

Another factor to consider is the orientation of the nitrate group. The combination $\pi_L^* \pm z^2_{Mn}$ must be sensitive to the orientation of the nitrate group in front of the z axis. This orientation is related to the torsion angle γ(ONOMn). When the nitrate group is perpendicular to the z axis (γ = 90°) (Figure 11) a good overlap between the π_L^* and the z^2_{Mn} orbital can be found, while for the other extreme when the nitrate ligand is aligned to the z axis (γ = 0° or 180°) the overlap vanishes.

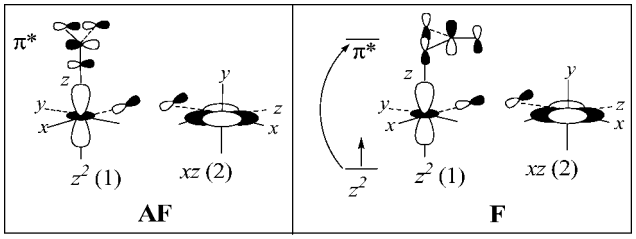

Figure 11. Schematic representation of the effect of the NO_3^- ligand in the z^2–xz antiferromagnetic contribution.

Then, for compound **5**, the small γ angle and short N–O distances could explain that the π_L^* orbital does not contribute to the z^2 orbital. In compound **1**, with 2-MeC_6H_4-COO bridges, the nitrate ligand shows a good overlap between the π_L^* orbital and the z^2_{Mn} orbital. The two combinations, $\pi_L^* \pm z^2_{Mn}$ show an important contribution of the nitrate and the manganese orbitals (39% Mn and 42% nitrate and 29% Mn and 63% nitrate). For compound **3**, with 2-FC_6H_4COO bridges, the nitrate ligand is placed more parallel to the z axis and the two MO's are more localized, one of them with a major contribution from the manganese ion (61% Mn and 23% nitrate) and the other one with a major contribution from the nitrate group (12% Mn and 82% nitrate). For the nitrate complex of compound **11** the higher energy orbital shows a major contribution from the π* of the nitrate ligand (60% of nitrate and 19% of z^2_{Mn})

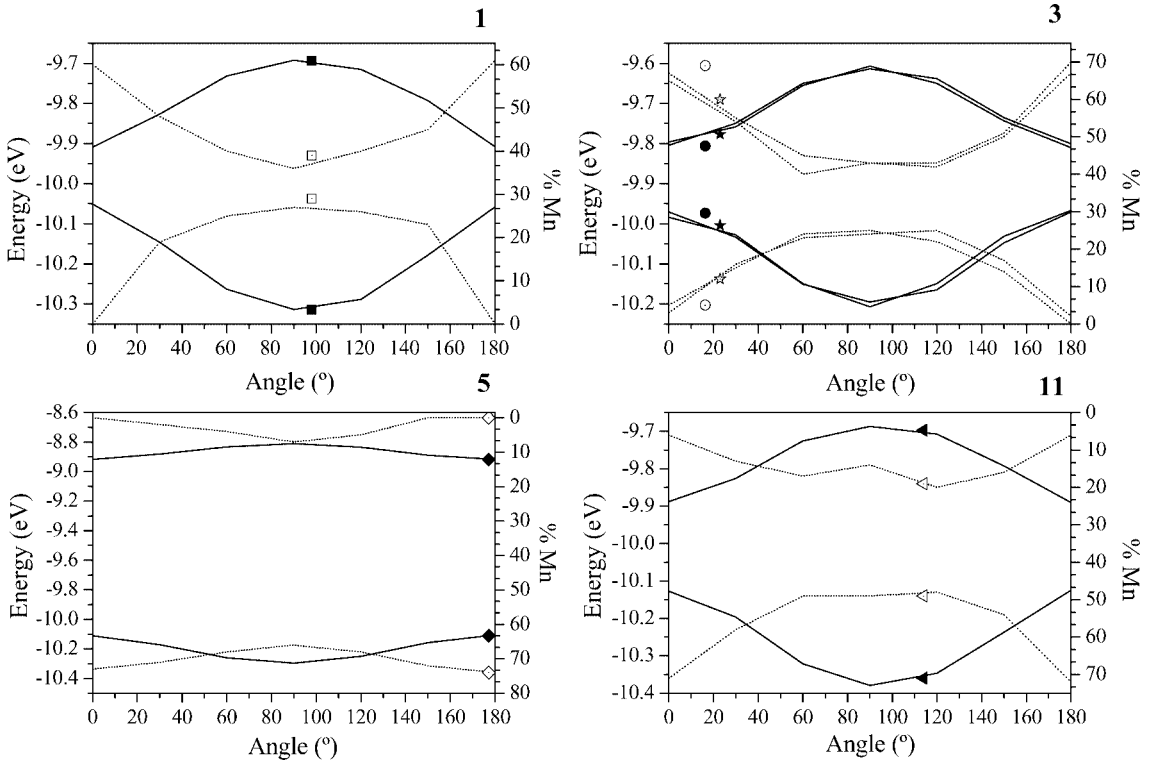

Figure 12. Energy of the $z^2 \pm \pi^*$ orbitals (solid line), and contribution of the Mn ions (%) to the MO (dotted line) as a function of the Mn–O–N–O angle (γ angle) for compounds **1** (top, left), **3** (top, right), **5** (bottom, left) and **11** (bottom, right). The filled symbols show the energy and the dotted symbols show the composition (% Mn) of the orbitals found for the real compounds (experimental values of γ, Table 6). For compound **3** the coordination of the two nitrates is considered.

while the lower energy orbital shows a major contribution from the z^2_{Mn} orbital (49%) and 31% of the π* orbital of the monodentate ligand.

Figure 12 shows the effect in the energy and composition of the $\pi_L^* \pm z^2_{Mn}$ orbitals by the variation of the Mn–O–N–O angle (γ), between 0–180°. This variation is not appreciable for compound **5**. For compounds **1**, **3** and **11** the modification of this torsion angle has an important effect. The major energy gap between the MO $\pi_L^*+z^2_{Mn}$ and $\pi_L^*-z^2_{Mn}$ orbitals was found for $\gamma \approx 90°$, and with this orientation a similar contribution of the π_L^* and z^2_{Mn} was found in all cases. Consequently, the nitrate ligand could act as a π-acid ligand, providing a means for the delocalization of the electronic density of the manganese z^2 orbital onto the ligand. This situation is enhanced if the nitrate ligand is placed perpendicular to the z axis. Then, the antiferromagnetic interactions $z^2(1)/xz(2)$ and $xy(1)/z^2(2)$ could diminish, and when the delocalization to the empty π* orbital of the nitrate ligand is important the ferromagnetic contribution could be increased. This could explain the minor antiferromagnetic interaction observed for the nitrate complexes **1** and **3** in comparison to their analogous compounds with perchlorate ligands.

On the other hand, the energy of the z^2 orbital decreases considerably by increasing the elongation in the z direction, therefore the antiferromagnetic interaction $z^2(1)/xz(2)$ and $xy(1)/z^2(2)$ could be more efficient; increases the antiferromagnetic contribution resulting in a more negative value for the overall coupling, as is observed for compounds **2**, **4**, **7**, **9** and **10**.

Conclusions

In this paper we reported the synthesis of four dinuclear Mn^{III} complexes with the general formula [{Mn(bpy)L}(μ-RCOO)$_2$(μ-O){Mn(bpy)L′}]X_{2-m} (RCOO = 2-MeC_6H_4COO and 2-FC_6H_4COO); these compounds show a labile position on each manganese ion, which could be occupied by different ligands: H_2O, NO_3^- or ClO_4^-. The magnetic properties are sensitive to the carboxylate bridges and the counteranion/monondentate ligand: compounds with 2-MeC_6H_4COO show much more antiferromagnetic coupling than compounds with 2-FC_6H_4COO, and perchlorate complexes show more of an antiferromagnetic interaction than the nitrate complexes. Several factors are being evaluated by Extended Hückel calculations and show that that the most important effect is the coordination of the nitrate ligand and their orientation, parallel to the z axis (small values of γ) or perpendicular to the z axis (γ close to 90°). This ligand could act as a π-acid ligand and then provide a new ferromagnetic means of interaction.

Experimental Section

Synthesis: All manipulations were performed under aerobic conditions. Organic reagents were used as received. Bu_4NMnO_4 was prepared as described in the literature.[19] The yield was calculated from the total available Mn.

Caution! Perchlorate salts of compounds containing organic ligands are potentially explosive. Only small quantities of these compounds should be prepared and handled behind protective shields.

[{Mn(bpy)L}(μ-2-RC$_6$H$_4$COO)$_2$(μ-O) {Mn(bpy)L′}]X$_{2-m}$, with R = CH$_3$ and X = NO$_3^-$ (1), ClO$_4^-$ (2), R = F and X = NO$_3^-$ (3), ClO$_4^-$ (4); L and L′ = H$_2$O or X: The four compounds were synthesized using the same procedure: 1.6 mmol of the benzoic derivative acid (0.22 g of 2-MeC_6H_4COOH or 0.23 g of 2-FC_6H_4COOH) was added to a solution containing the Mn^{II} salt (1.28 mmol) in MeCN, $Mn(NO_3)_2{\cdot}4H_2O$ (0.32 g) or $Mn(ClO_4)_2{\cdot}6H_2O$ (0.45 g). Bu_4NMnO_4 (0.11 g, 0.32 mmol) dissolved in MeCN was then added to the solution, which immediately turned dark brown. Finally, a MeCN solution of 2,2′-bipyridine (0.25 g, 1.6 mmol) was added and the resulting solution was stirred for some minutes. The total volume for the nitrate compounds (**1** and **3**) was 100 mL, and was 30 mL for the perchlorate compounds (**2** and **4**). Small dark crystals were obtained from the nitrate solutions when they were left undisturbed in the refrigerator for several days (compounds **1** and **3**). For the compounds with perchlorate anions suitable X-ray diffraction crystals were obtained in the presence of CH_2Cl_2. The compound with the 2-$MeC_6H_4COO^-$ bridging ligand crystallized from the mother MeCN solution mixed with CH_2Cl_2 (1:1), which was layered with hexanes and left undisturbed at room temperature. While for the compound with 2-$FC_6H_4COO^-$ bridges, the mother MeCN solution was kept inside a container with an atmosphere of CH_2Cl_2 and after several days at room temperature crystals of compound **4** were obtained.

Compound 1, [{Mn(bpy)(H$_2$O)}(μ-2-MeC$_6$H$_4$COO)$_2$(μ-O){Mn(NO$_3$)(bpy)}]NO$_3$·H$_2$O: Yield 0.38 g (ca. 56%). $C_{36}H_{32}Mn_2N_6O_{12}{\cdot}H_2O$ (868.56): calcd. C 49.78, H 3.95, N 9.68; found C 49.9, H 3.8, N 9.7. IR (KBr): $\tilde{\nu}_{max}$ = 1609 (m, COO), 1384 (vs., COO + NO_3), 730 (m, Mn_2O) cm^{-1}.

Compound 2, [{Mn(bpy)(H$_2$O)}$_2$(μ-2-MeC$_6$H$_4$COO)$_2$(μ-O)][{Mn(ClO$_4$)(bpy)}$_2$(μ-2-MeC$_6$H$_4$COO)$_2$(μ-O)](ClO$_4$)$_2$·CH$_2$Cl$_2$: Yield 0.44 g (ca. 58%). $C_{72}H_{64}Cl_4Mn_4N_8O_{28}{\cdot}CH_2Cl_2{\cdot}$(1935.81): calcd. C 45.29, H 3.44, N 5.79; found C 45.5, H 3.4, N 5.9. IR (KBr): $\tilde{\nu}_{max}$ = 1604 (m COO), 1384 (vs., COO), 1156 (vs., ClO_4) 1150 (vs., ClO_4), 1031 (vs. ClO_4), 730 (m, Mn_2O) cm^{-1}.

Compound 3, [{Mn(bpy)(H$_2$O)}(μ-2-FC$_6$H$_4$COO)$_2$(μ-O){Mn(NO$_3$)(bpy)}]NO$_3$·H$_2$O: Yield 0.44 g (ca. 63%). $C_{34}H_{26}F_2Mn_2N_6O_{12}{\cdot}2H_2O$ (894.51): calcd. C 45.65, H 3.38, F 4.25, N 9.40; found C 45.6, H 3.2, F 4.2, N 9.6. IR (KBr): $\tilde{\nu}_{max}$ = 1610 (s, COO), 1384 (vs., COO + NO_3), 730 (w, Mn_2O) cm^{-1}.

Compound 4, [{Mn(bpy)(H$_2$O)}(μ-2-FC$_6$H$_4$COO)$_2$(μ-O){Mn(ClO$_4$)(bpy)}]ClO$_4$: Yield 0.42 g (ca. 57%). $C_{34}H_{26}Cl_2F_2Mn_2N_4O_{14}{\cdot}H_2O$ (951.38): calcd. C 42.92, H 2.97, Cl 7.45, F 3.99, N 5.89; found C 43.0, H 2.7, Cl 7.5, F 4.0, N 5.8. IR (KBr): $\tilde{\nu}_{max}$ = 1611 (vs., COO), 1383 (vs., COO), 1146 (vs., ClO_4), 1119 (vs., ClO_4), 1089 (vs., ClO_4), 725 (m, Mn_2O) cm^{-1}.

Physical Measurements: Elemental analyses of C, H, Cl, F and N were carried out by the "Serveis Científico-Tècnics" of the Universitat de Barcelona. Infrared spectra (4000–400 cm^{-1}) were recorded from KBr pellets with a Nicolet Impact 400 FT-IR spectrometer. Magnetic susceptibility measurements were performed with a Manics-DSM8 susceptometer equipped with an Oxford Instruments helium cryostat, working down to 4.2 K, and carried out at the "Servei de Magnetoquímica" (Universitat de Barcelona). The field used was in the interval 6000–8000 G. For the ferromagnetic compound the magnetic susceptibility (between 300–2 K, at

Table 7. Crystallographic data for **1**–**4**.

	1	**2**	**3**	**4**
Formula	$C_{40}H_{44}Mn_2N_8O_{15}$	$C_{73}H_{66}Cl_6Mn_4N_8O_{28}$	$C_{34}H_{28}F_2Mn_2N_6O_{13}$	$C_{36}H_{30}Cl_6F_2Mn_2N_4O_{14}$
Formula mass [g mol^{-1}]	986.70	1935.80	876.50	1103.22
Crystal system	triclinic	triclinic	monoclinic	triclinic
Space group	$P\bar{1}$	$P\bar{1}$	$P2_1/n$	$P\bar{1}$
a [Å]	9.9202(1)	15.7038(16)	9.9948(1)	10.096(2)
b [Å]	15.663	17.2438(17)	25.2891(2)	14.229(3)
c [Å]	17.0380(2)	17.9876(17)	16.5490(2)	16.496(3)
α [°]	108.401(1)	109.245(2)	90	66.66(3)
β [°]	105.429(1)	107.223(2)	100.19	89.652(16)
γ [°]	103.829(1)	107.016(2)	90	84.490(16)
V [Å^3]	2265.45(4)	3959.9(7)	4116.99(7)	2164(8)
Z	2	2	4	2
T [K]	173(2)	173(2)	298(2)	173(2)
$\rho_{calcd.}$ [g cm^{-3}]	1.444	1.623	1.414	1.693
$\mu_{calcd.}$ [mm^{-1}]	0.633	0.914	0.689	1.033
$F(000)$	978	1972	1784	1112
Transmission factors (max., min.)	0.9117, 0.7238	0.8751, 0.7839	0.7701, 0.7245	0.8201, 0.6262
Θ range for data collection [°]	1.36 to 28.28	1.33 to 26.37	1.49 to 28.32	1.35 to 28.41
Total reflections measured	15735	23472	27341	11907
Independent reflections, R_{int}	10819, 0.0318	15845, 0.0612	9902, 0.0766	9461, 0.1019
Completeness to Θ_{max}	96.2%	97.8%	96.4%	86.9%
Parameters refined, restrains	571, 21	1099, 0	616, 31	577, 0
R_1[a] [$I > 2\sigma(I)$]	0.0672	0.0687	0.0769	0.1170
wR_2[b] [$I > 2\sigma(I)$]	0.1937	0.1223	0.2152	0.2795
R_1[a] [all data]	0.0970	0.1765	0.1284	0.1971
wR_2[b] [all data]	0.2170	0.1592	0.2382	0.3287
Goodness of fit on F^2	1.044	0.977	1.025	0.890
Largest diff. peak and hole [e A^{-3}]	1.350 and –0.735	0.747 and –0.860	0.784 and –0.640	1.177 and –2.046

[a] $R_1 = \Sigma||F_o| - |F_c|| / \Sigma|F_o|$. [b] $wR_2 = \{\Sigma[w(F_o^2 - F_c^2)^2] / \Sigma[w(F_o^2)^2]\}^{1/2}$.

1000 G) and the magnetization (at 2 K between 0–50000 G) were measured with a SQUID magnetometer, Quantum Design Magnetometer, model MPMP. Pascal's constants were used to estimate the diamagnetic corrections for each compound. The fits were performed by minimizing the function $R = \Sigma(\chi_M \cdot T_{exp} - \chi_M \cdot T_{calcd})^2 / \Sigma(\chi_M \cdot T_{exp})^2$. All the samples were prepared by crushing the crystalline products.

Crystallographic Measurements: A green plate crystal ($0.50 \times 0.50 \times 0.15$ mm) of [{Mn(bpy)(H_2O)}(μ-2-$MeC_6H_4COO)_2$(μ-O){Mn(NO_3)(bpy)}]$NO_3 \cdot 1.5CH_3CN \cdot 2H_2O$ (**1**), a brown block crystal ($0.28 \times 0.15 \times 0.15$ mm) of [{Mn(bpy)(H_2O)}$_2$-(μ-2-$MeC_6H_4COO)_2$(μ-O)][{Mn(ClO_4)(bpy)}$_2$(μ-2-$MeC_6H_4COO)_2$-(μ-O)]$(ClO_4)_2 \cdot 0.5CH_2Cl_2$ (**2**), a black block crystal ($0.50 \times 0.50 \times 0.40$ mm) of [{Mn(bpy)(H_2O)}(μ-2-$FC_6H_4COO)_2$(μ-O){Mn(NO_3)(bpy)}]-$NO_3 \cdot H_2O$ (**3**) and a dark green block crystal ($0.50 \times 0.25 \times 0.20$ mm) of [{Mn(bpy)(H_2O)}(μ-2-$FC_6H_4COO)_2$(μ-O){Mn(ClO_4)(bpy)}]-$ClO_4 \cdot 2CH_2Cl_2$ (**4**) were chosen for X-ray diffraction experiments. The unit cell and intensity data were measured with a Bruker SMART CCD area detector single-crystal diffractometer with graphite monochromated Mo-K_α radiation (λ = 0.71073 Å) operating at 50 kV and 30 mA. A total of 1271 frames of intensity data were collected over a hemisphere of the reciprocal space by a combination of three exposure sets. Each frame covered 0.3° in ω and the first 50 frames were recollected at the end of the data collection to monitor crystal decay. Absorption corrections were applied using the SADABS program.[20] The structures were solved using the Bruker SHELXTL-PC software[21] by direct methods and refined by full-matrix least-squares methods on F^2. Hydrogen atoms were included in calculated positions and refined in the riding mode except those of the water molecules that were located on residual density maps, and their positions were then fixed and refined in the riding mode. All non-hydrogen atoms were refined anisotropically. Crystal data collection and refinement parameters are given in Table 7. Further details, concerning disorder for example, are given in the crystallographic CIF files. CCDC-288243 to -288246 contain the supplementary crystallographic data for this paper. These data can be obtained free of charge from The Cambridge Crystallographic Data Centre via www.ccdc.cam.ac.uk/datarequest/cif.

Acknowledgments

The authors thank the Ministerio de Educación y Ciencia for financial support (Ramon y Cajal research contract and grants BQ 2003-00538 and CTQ 2005-08123-C02-02/BQU). Thanks also go to X. Solans for help with the crystallographic ressolution.

[1] B. C. Dave, R. S. Czernuszewickz, *Inorg. Chim. Acta* **1998**, *281*, 25.
[2] R. Ruiz, C. Sangregorio, A. Caneschi, P. Rossi, A. B. Gaspar, J. A. Real, M. C. Muñoz, *Inorg. Chem. Commun.* **2000**, *3*, 361.
[3] K. R. Reddy, M. V. Rajasekharan, S. Sukumar, *Polyhedron* **1996**, *15*, 4161.
[4] B. Albela, M. Corbella, J. Ribas, *Polyhedron* **1996**, *15*, 91.
[5] M. Corbella, R. Costa, J. Ribas, P. H. Fries, J. M. Latour, L. Ohrstrom, X. Solans, V. Rodríguez, *Inorg. Chem.* **1996**, *35*, 1857.
[6] J. B. Vincent, K. Folting, C. J. Huffman, G. Christou, *BioChem. Soc. Trans.* **1988**, *16*, 822.
[7] J. B. Vincent, H. L. Tsai, A. G. Blackman, S. Wang, P. D. Boyd, K. Folting, J. C. Huffman, E. B. Lobkovsky, D. N. Hendrickson, G. Christou, *J. Am. Chem. Soc.* **1993**, *115*, 12353.
[8] G. Fernández, M. Corbella, M. Alfonso, H. Stoeckli-Evans, I. Castro, *Inorg. Chem.* **2004**, *43*, 6684.
[9] S. Ménage, J.-J. Girerd, A. Gleizes, *J. Chem. Soc., Chem. Commun.* **1988**, 431.

[10] C. Chen, H. Zhu, D. Huang, T. Wen, Q. Liu, D. Liao, J. Cui, *Inorg. Chim. Acta* **2001**, *320*, 159.
[11] K. Wieghardt, U. Bossek, D. Ventur, J. Weiss, *J. Chem. Soc., Chem. Commun.* **1985**, 347.
[12] K. Wieghardt, U. Bossek, B. Nuber, J. Weiss, J. Bonvoisin, M. Corbella, S. E. Vitols, J. J. Girerd, *J. Am. Chem. Soc.* **1988**, *110*, 7398.
[13] C. Bolm, N. Meyer, G. Raabe, T. Weyhermüller, E. Bothe, *Chem. Commun.* **2000**, 2435.
[14] J. E. Sheats, R. S. Czernuszewicz, G. C. Dismukes, A. L. Rheingold, V. Petrouleas, J. A. Stubbe, W. H. Armstrong, R. H. Beer, S. J. Lippard, *J. Am. Chem. Soc.* **1987**, *109*, 1435.
[15] F. J. Wu, D. M. Kurtz Jr, K. S. Hagen, P. D. Nyman, P. G. Debrunner, V. A. Vankai, *Inorg. Chem.* **1990**, *29*, 5174.
[16] R. Hotzelmann, K. Wieghardt, U. Flörke, H.-J. Haupt, D. C. Weatherburn, J. Bonvoisin, G. Blondin, J.-J. Girerd, *J. Am. Chem. Soc.* **1992**, *114*, 1681.
[17] O. Kahn, *Molecular Magnetism*, Wiley-VCH, **1993**.
[18] C. Mealli, D. Proserpio, *J. Chem. Educ.* **1990**, *67*, 399.
[19] T. Sala, M. V. Sargent, *J. Chem. Soc., Chem. Commun.* **1978**, 253.
[20] G. M. Sheldrick, *SADABS, Program for Empirical Absorption Correction of Area Detector Data*, University of Göttingen, Germany, **1996**. On the basis of the method by Robert Blessing: R. H. Blessing, *Acta Crystallogr., Sect. A* **1995**, *51*, 33.
[21] M. Sheldrick, *SHELXTL-PC, Program for Crystal Structure Solution*, University of Göttingen: Göttingen, Germany, **1997**.

Received: July 28, 2006
Published Online: February 13, 2007

